

# Adeno-Associated Virus Gene Repair Corrects a Mouse Model of Hereditary Tyrosinemia *In Vivo*

Nicole K. Paulk,<sup>1\*</sup> Karsten Wursthorn,<sup>1,2\*</sup> Zhongya Wang,<sup>1</sup> Milton J. Finegold,<sup>3</sup> Mark A. Kay,<sup>4</sup> and Markus Grompe<sup>1,5</sup>

Adeno-associated virus (AAV) vectors are ideal for performing gene repair due to their ability to target multiple different genomic loci, low immunogenicity, capability to achieve targeted and stable expression through integration, and low mutagenic and oncogenic potential. However, many handicaps to gene repair therapy remain. Most notable is the low frequency of correction *in vivo*. To date, this frequency is too low to be of therapeutic value for any disease. To address this, a point-mutation–based mouse model of the metabolic disease hereditary tyrosinemia type I was used to test whether targeted AAV integration by homologous recombination could achieve high-level stable gene repair *in vivo*. Both neonatal and adult mice were treated with AAV serotypes 2 and 8 carrying a wild-type genomic sequence for repairing the mutated *Fab* (fumarylacetoacetate hydrolase) gene. Hepatic gene repair was quantified by immunohistochemistry and supported with reverse transcription polymerase chain reaction and serology for functional correction parameters. Successful gene repair was observed with both serotypes but was more efficient with AAV8. Correction frequencies of up to  $10^{-3}$  were achieved and highly reproducible within typical dose ranges. In this model, repaired hepatocytes have a selective growth advantage and are thus able to proliferate to efficiently repopulate mutant livers and cure the underlying metabolic disease. **Conclusion:** AAV-mediated gene repair is feasible *in vivo* and can functionally correct an appropriate selection-based metabolic liver disease in both adults and neonates. (HEPATOLOGY 2010;51: 1200-1208.)

Gene therapy is a promising means to cure many monogenic diseases. However, traditional gene therapies are best suited to treat diseases of deficient or absent gene products rather than those diseases

caused by aberrantly functioning proteins. Even now, gene therapy efforts remain focused on gene addition strategies using full-length complementary DNA (cDNA) cassettes for the mutated gene of interest, driven by promoter and enhancer sequences.<sup>1</sup> Despite many advances, gene addition approaches with adeno-associated virus (AAV) are limited by transient and unregulated expression,<sup>2</sup> highly random integrations,<sup>3</sup> transgene silencing,<sup>4</sup> and increased mutagenic and oncogenic risks.<sup>5</sup> Not all protein-coding genes have open reading frames small enough to fit within the low coding capacity of AAV (4.7 kb), thus, this type of gene therapy is not applicable for all disorders.<sup>6</sup>

Gene repair offers a solution to these drawbacks, where patient genomes are manipulated *in vivo* using site-specific recombination to actually correct the underlying mutation. Contrary to more widely used gene addition paradigms, gene repair restores gene function within the context of all endogenous regulatory elements, thereby eliminating potential problems with inadequate or inappropriate expression. Different vehicles have been utilized for performing gene repair including single-strand oligonucleotides,<sup>7-9</sup> triplex-forming oligonucleotides,<sup>10</sup> RNA-DNA hybrids,<sup>11,12</sup> small fragment DNA, and AAV.<sup>13-15</sup> Of these, AAV has emerged as the most promising. Nu-

---

Abbreviations: AAV, adeno-associated virus; AST, aspartate aminotransferase; dGE, diploid genome equivalent; FAH, fumarylacetoacetate hydrolase; GAPDH, glyceraldehyde 3-phosphate dehydrogenase; hAAT, human alpha-1 antitrypsin; HTI, hereditary tyrosinemia type I; LD-PCR, long-distance polymerase chain reaction; NTBC, 2-(2-nitro-4-trifluoro-methylbenzol)-1,3-cyclohexanedione; RT-PCR, reverse transcription polymerase chain reaction; vg, vector genome.

From the <sup>1</sup>Oregon Stem Cell Center, <sup>2</sup>Papé Pediatric Institute, Oregon Health and Science University, Portland, OR; <sup>3</sup>Gastroenterology, Hepatology and Endocrinology Clinic, Hannover Medical School, Hannover, Germany; <sup>4</sup>Department of Pathology, Texas Children's Hospital, Houston, TX; and <sup>5</sup>Department of Pediatrics and Genetics, Stanford University, Stanford, CA.

Received January 8, 2009; accepted November 22, 2009.

\*These authors contributed equally to this work.

This work was supported by grants from the National Institute of Diabetes and Digestive and Kidney Diseases to M.G. (ROI-DK48252) and the National Cancer Institute to N.P. (F31CA130116). The funding organizations played no role in experimental design, data analysis, or manuscript preparation.

Address reprint requests to: Markus Grompe, Oregon Health and Science University, Oregon Stem Cell Center, 3181 SW Sam Jackson Park Road, Mail Code: L321, Portland, OR 97203. E-mail: grompem@ohsu.edu; fax: 503-418-5044.

Copyright © 2009 by the American Association for the Study of Liver Diseases.

Published online in Wiley InterScience (www.interscience.wiley.com).

DOI 10.1002/hep.23481

Potential conflict of interest: Nothing to report.

merous *in vitro* studies have shown AAV capable of correcting various types of mutations (insertions, deletions, substitutions) by vector-mediated homologous recombination.<sup>16,17</sup> AAV vectors engineered to perform gene repair have the ability to target multiple different genomic loci, show both targeted and stable expression through integration, and have an increased number of applicable human diseases.<sup>18</sup> Single-stranded AAV genomes modulate gene repair by integrating site-specifically via homologous recombination and targeting only the disease-causing mutation for replacement with wild-type sequence.<sup>19</sup> Gene repair is best suited to correct point-mutation-based diseases that need only one or few nucleotides corrected to restore normal gene expression. This is key, because point mutations are the most frequent genetic abnormality and source of acquired genetic disease.<sup>20</sup>

To demonstrate targeted hepatic gene repair *in vivo* for a clinically pertinent disease gene, a hereditary tyrosinemia type I (HTI) mouse model (*Fah*<sup>5981SB</sup>) was used. HTI is a fatal genetic disease caused by deficiency of fumarylacetoacetate hydrolase (FAH), the terminal enzyme in the tyrosine catabolic pathway.<sup>21</sup> When a FAH deficiency exists, toxic metabolites such as fumarylacetoacetate accumulate in hepatocytes and renal proximal tubules causing death in a cell-autonomous manner.<sup>22</sup> Toxic metabolite accumulation can be blocked by 2-(2-nitro-4-trifluoromethylbenzoyl)-1,3-cyclohexanedione (NTBC) administration, a pharmacological inhibitor that blocks the pathway upstream of FAH.<sup>23</sup> The *Fah*<sup>5981SB</sup> mouse is ideal to study gene repair, because it is point-mutation-based and fully recapitulates the human disease on an accelerated time scale. Strong positive selection for FAH<sup>+</sup> cells in the HTI mouse liver has been demonstrated<sup>24</sup> and was exploited for *in vivo* selection of corrected hepatocytes following gene repair. In this system, when AAV vectors containing genomic *Fah* sequence (hereafter referred to as AAV-*Fah*) are administered to *Fah*<sup>5981SB</sup> mice, only corrected FAH-positive (FAH<sup>+</sup>) hepatocytes that have undergone integration by homologous recombination can survive and repopulate the liver. The outcome is formation of corrected FAH<sup>+</sup> nodules and loss of unintegrated episomal vector genomes. In both neonatal and adult mice treated with AAV-*Fah*, gene repair restored proper gene and protein expression and cured the underlying HTI phenotype. These results demonstrate proof-of-principle that an appropriate monogenic liver disease can be corrected by AAV-mediated gene repair *in vivo*.

## Materials and Methods

**Mouse Strains and Animal Husbandry.** The *Fah*<sup>5981SB</sup> mouse<sup>25</sup> models HTI by bearing a single *N*-

ethyl-*N*-nitrosourea-induced point mutation in the final nucleotide of exon 8 within the *Fah* gene.<sup>26</sup> This point mutation creates a premature downstream stop codon and exon 8 loss, ultimately leading to formation of truncated, unstable FAH protein that is degraded. *Fah*<sup>5981SB</sup> mice die as neonates from acute liver failure if NTBC is not continually administered in the drinking water. NTBC treatment at 4 mg/mL rescues the phenotype and prevents acute hepatocellular and renal injury. Discontinuation of NTBC provides an accurate model of HTI. Mice develop liver and renal disease within 10 days, which progresses to full end-stage liver disease and death within 6-8 weeks.<sup>27</sup> The mice have been backcrossed 10 generations onto a C57BL6 background. The Institutional Animal Care and Use Committee of Oregon Health and Science University approved all procedures and mouse experiments.

**Plasmid Construction.** *Mus musculus* bacterial artificial chromosome (BAC) clone RP23-121N17 from chromosome 7 (Invitrogen) was used as a template for the 4.5-kb long-distance polymerase chain reaction (LD-PCR) amplification of sequence homologous to the region centered on the point mutation in exon 8 of murine *Fah* (RefSeq NM\_010176, chr7:84461356-84481935). Forward primer introducing *NotI*: 5'-GCGGCCGCT-TCCCAGGGTTTTTGTGTT-3'; reverse primer: 5'-AGCCCCACTGACAGCTACAGCT-3'. The PCR resulted in a 4.5-kb product with an introduced 5'-*NotI* restriction site that allowed cloning into an AAV plasmid backbone as previously described.<sup>28</sup>

**Sequencing.** DNA sequencing was performed with an ABI-Prism 3130xl Genetic Analyzer (Applied Biosystems Inc., Foster City, CA) at the Vollum Sequencing Core (Portland, OR). DNA sequences were aligned with MacVector software.

**Neonatal Vector Administration.** For time course studies, d3 *Fah*<sup>5981SB</sup> neonates were injected with 1 × 10<sup>11</sup> (AAV2-*Fah*) or 2 × 10<sup>11</sup> (AAV8-*Fah*) vector genome (vg) in 10 μL volume by intravenous facial vein injection.<sup>29</sup> Littermate controls were similarly injected with 1 × 10<sup>11</sup> to 2 × 10<sup>11</sup> vg of an irrelevant serotype-matched control vector; either AAV2-*hAAT*,<sup>30</sup> or AAV8-*GFP*.<sup>31</sup> All mice were maintained on NTBC throughout. Livers were harvested at 1, 2, or 4 weeks after treatment. For dose-response studies, d3 *Fah*<sup>5981SB</sup> neonates were injected with four doses ranging from 3 × 10<sup>8</sup> to 3 × 10<sup>11</sup> vg (in 10 μL volume) of each serotype by intravenous facial vein injection. All mice were maintained on NTBC throughout. Livers were harvested 2 weeks after treatment. For stable integration studies, d3 *Fah*<sup>5981SB</sup> neonates were injected with AAV2-*Fah* at 1 × 10<sup>11</sup> vg in 10 μL volume by intravenous facial vein injection. Litter-

mate controls were similarly injected with isotonic NaCl solution. Mice were maintained on NTBC until weaning and then withdrawn to select for corrected hepatocytes. Eleven weeks after treatment, a two-thirds partial hepatectomy was performed to induce liver regeneration.<sup>32</sup> Livers were harvested >12 weeks after surgery. For random integration studies, d3 *Fah*<sup>5981SB</sup> neonates were coinjected with  $4 \times 10^{10}$  vg of both AAV8-*Fah* and AAV8-*hAAT* (in 10  $\mu$ L volume) by intravenous facial vein injection. Mice were maintained on NTBC until weaning and then withdrawn to select for corrected hepatocytes. Serum (for liver function tests) and liver tissue were collected at harvest.

**Adult Vector Administration.** Adult *Fah*<sup>5981SB</sup> mice (age 8-12 weeks) were injected with  $1 \times 10^{11}$  vg of AAV8-*Fah* (in 100  $\mu$ L volume) by intravenous tail vein injection. Age-matched littermate controls were similarly injected with isotonic NaCl solution. Mice were placed on NTBC as needed. Serum and liver tissue were harvested >12 weeks after treatment.

**Liver Immunohistochemistry.** In both adult and neonatal experiments, a minimum of two liver sections were analyzed per mouse and evaluated for the number of FAH<sup>+</sup> cell clusters, each representing the clonal expansion of a single corrected hepatocyte. Clonal frequencies, correction factors, hepatocyte counts, fixation, and immunohistochemistry protocols were done as described.<sup>33</sup> Quantitation was performed by two separate, blinded investigators.

**Statistical Analysis.** Experimental results were analyzed for significance by applying a student 2-tailed *t*-test assuming equal variance. *P* values <0.05 were considered statistically significant.

**Vector Preparation.** AAV vector preparation and titrating were performed according to standard AAV protocols as described.<sup>34</sup>

**Transplantation.** For serial transplantation surgeries, livers were isolated from corrected mice and  $3 \times 10^5$  to  $5 \times 10^5$  random hepatocytes were injected intrasplenically at 100  $\mu$ L volume into *Fah*<sup>5981SB</sup> recipient mice as described.<sup>35</sup>

***Fah* Quantitative Reverse Transcription PCR.** Total RNA was isolated from randomly dissected liver tissue with an RNeasy Mini kit (Qiagen). The cDNA was produced with a Superscript III First-Strand Synthesis kit (Invitrogen). PCR was performed on an iCycler (Bio-Rad Laboratories). Reverse transcription (RT) reaction (100 ng) was subjected to two-step PCR amplification under the following conditions: 1 cycle 95°C  $\times$  3 minutes, followed by 45 cycles of 95°C  $\times$  15 seconds and 68°C  $\times$  50 seconds. Primer sequences: *Fah* forward: 5'-AGAAGT-TACTGTCTGCCAGCCAAG-3'; *Fah* reverse: 5'-

GAGGACCATCCCGAAAATGTG-3'; glyceraldehyde 3-phosphate dehydrogenase (*Gapdh*) forward: 5'-CCACCCCAGCAAGGACTG-3'; *Gapdh* reverse 5'-GCTCCCTAGGCCCTCCTGT-3'. All samples were subjected to  $\pm$  RT controls and results were normalized to *Gapdh* expression.

***hAAT* Copy Number Quantitative PCR.** Total DNA was isolated from randomly dissected liver tissue with a MasterPure DNA Purification kit (Epicentre Biotechnologies). PCR was performed on an iQ5 Multicolor Real-Time PCR (Bio-Rad), using the iQ5 Standard Edition Software, version 2.0. Genomic DNA (10 ng) was subjected to a two-step PCR amplification under the following conditions: 1 cycle 95°C  $\times$  3 minutes, followed by 45 cycles of 95°C  $\times$  15 seconds and 68°C  $\times$  40 seconds. Primer sequences: *hAAT* forward: 5'-TCCTGGGTCAACTGGGCATC-3'; *hAAT* reverse: 5'-CAGGGGTGCCTCCTCTGTGA-3'; *Gapdh* forward: 5'-CCACCCCAGCAAGGACTG-3'; *Gapdh* reverse 5'-GCTCCCTAGGCCCTCCTGT-3'. Dilutions of *hAAT* plasmid into mouse genomic DNA were used to generate copy number standards. Results were normalized to *Gapdh* expression.

## Results

**Target Vector Design.** In *Fah*<sup>5981SB</sup> mice, a single point mutation (G $\rightarrow$ A transversion) at the terminal nucleotide of *Fah* exon 8 leads to mis-splicing and exon-8 deletion from the messenger RNA (mRNA). Several important criteria derived from the literature<sup>18</sup> were considered for the design of the gene repair vector to correct the *Fah*<sup>5981SB</sup> point mutation (Fig. 1A). First, the vector should not contain elements needed for driving gene expression such as promoters, enhancers, or cDNA expression cassettes. Second, the fidelity and length of homology should be maximized with the packaging capacity of AAV (4.7 kb) being the limit. Third, the position of the nucleotide targeted for repair should be at the center of the homology. A 4.5-kb PCR product homologous to murine *Fah* was cloned into an AAV plasmid backbone and verified by DNA sequencing. Recombinant AAV-*Fah* of serotypes 2 and 8 were produced and administered to *Fah*<sup>5981SB</sup> mice as neonates or adults. Correction of the point mutation by homologous recombination (Fig. 1B) leads to normal *Fah* gene and protein expression.

***AAV-Fah* Mediates Stable Gene Repair In Vivo.** The evaluation of homologous recombination as a strategy for gene repair has traditionally relied on detecting alterations in reporter sequences rather than correcting a disease phenotype. Given the selective advantage of

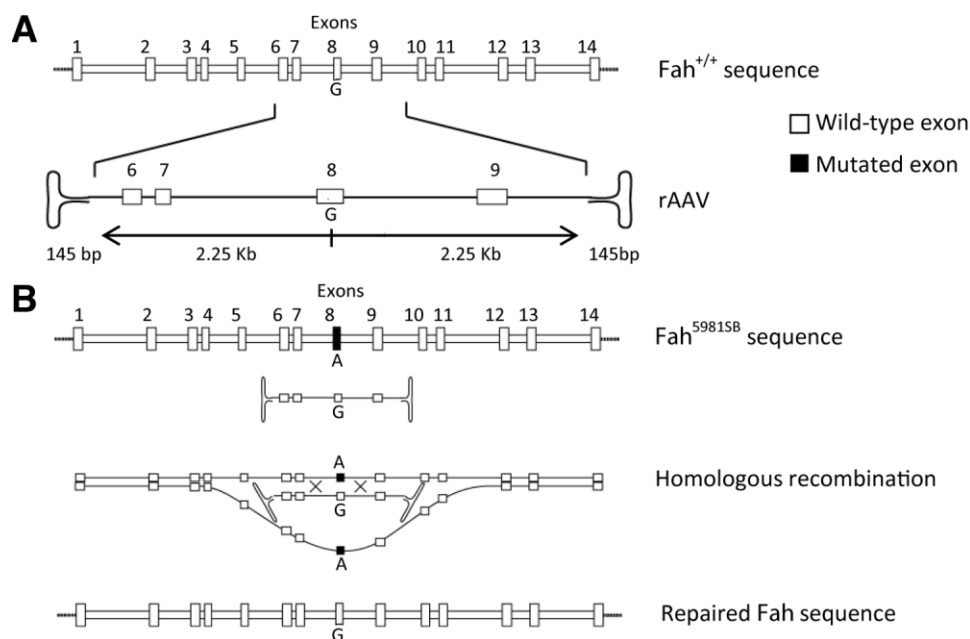


Fig. 1. AAV vector design and genomic organization of murine *Fah*. (A) A 4.5-kb genomic DNA fragment homologous to murine *Fah* was cloned into an AAV plasmid backbone and verified by DNA sequencing. The position of the nucleotide needed to perform repair was centered within two 2.25-kb homology arms. (B) Mechanism of AAV-mediated homologous recombination. Wild-type *Fah* has a guanine (G) as the terminal nucleotide of exon 8. In  $Fah^{5981SB}$  mice, a G→A transversion occurs at this position leading to mis-splicing and exon-8 deletion. Gene repair of the mutated *Fah* genomic sequence by AAV-mediated homologous recombination corrects the point mutation and restores proper *Fah* gene expression.

FAH<sup>+</sup> hepatocytes in the HTI liver,  $Fah^{5981SB}$  mice can be used to study the clinical significance of AAV-mediated gene repair by homologous recombination. Four d3  $Fah^{5981SB}$  neonates were intravenously injected with  $1 \times 10^{11}$  vg of AAV2-*Fah* and kept on NTBC until weaning, followed by NTBC withdrawal to select for corrected hepatocytes. Two control groups were injected with isotonic NaCl solution. Control group I (n = 3) did not receive a course of NTBC post-weaning, continued to lose weight and died. Control group II (n = 2) did receive one course of NTBC post-weaning but failed to maintain a healthy weight and died. AAV-treated mice began to stabilize in weight at 8 weeks after treatment, suggesting the onset of sufficient liver function. At age 11 weeks, a two-thirds partial hepatectomy was performed to induce liver regeneration and subsequent episomal AAV loss. Continued clinical improvement following partial hepatectomy strongly suggested stable gene repair at the *Fah* locus. FAH immunohistochemistry showed >50% FAH<sup>+</sup> hepatocytes in section overviews (Fig. 2A). The numbers of detectable liver nodules ranged from 21–47 per 50 mm<sup>2</sup> section in treated mice and were never detected in controls. Nodules represent the clonal expansion of a single corrected hepatocyte, thus nodule frequency must be corrected for nodule size. For this experiment, the correction factor was estimated to be fourteen. After correction, the initial gene repair frequency ranged from

1/6,300 to 1/11,600 hepatocytes and was within the expected range from previous experiments<sup>15</sup> where selection with NTBC did not apply.

To demonstrate that FAH staining was not artifactual and that proper *Fah* gene expression had indeed been restored, *Fah* RT-PCR was performed on RNA from treated livers. The presence of correctly spliced mRNA was demonstrated in all treated mice (Fig. 2B). To further demonstrate the stability of correction,  $3 \times 10^5$  random hepatocytes from a corrected mouse were serially transplanted into four secondary adult  $Fah^{5981SB}$  recipients. Serial transplantation is another means to induce hepatocyte turnover and eliminate episomal AAV genomes.<sup>35</sup> Serial transplant recipients had successful engraftment and displayed clinical improvement, whereas untransplanted controls showed continuous weight loss and died. FAH immunohistochemistry from livers of serial transplant recipients had extensive hepatocellular FAH staining, further demonstrating stability of the gene repair (Fig. 2A).

**Time course comparison of AAV8-*Fah* and AAV2-*Fah*.** AAV8 is the preferred serotype for liver transduction because of its strong hepatic tropism, rapid capsid disassembly and genome release.<sup>36</sup> In contrast, although AAV2 has been shown to transduce liver, it is characterized by slow capsid disassembly and genome release. To address the question whether AAV serotypes 8 and 2 have



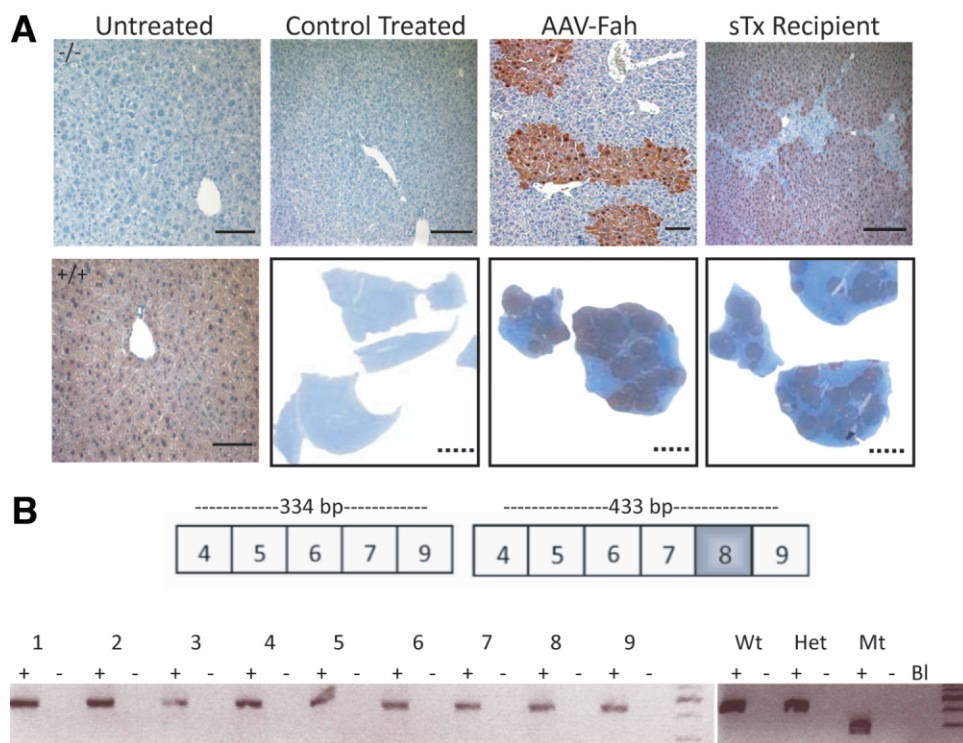


Fig. 2. AAV can mediate stable gene repair *in vivo*. (A) Liver immunohistology and whole-mount staining for FAH. In the top row from left to right, liver sections are from untreated mice (wild-type [ $+/+$ ] or  $Fah^{5981SB}$  [ $-/-$ ]); mock-injected  $Fah^{5981SB}$  mice; AAV-*Fah* treated  $Fah^{5981SB}$  mice; and  $Fah^{5981SB}$  mice after serial transplantation (sTx) with hepatocytes from a previously corrected mouse. Bottom row: Left panel shows wild-type liver as positive control for *Fah*. The following three panels are low-magnification overviews of liver sections. The second from left panel is from a mock-injected mouse and shows no FAH staining, whereas the two panels at right display multiple brown FAH<sup>+</sup> nodules after AAV-*Fah* injection. Scale bars: solid = 100  $\mu$ m; dotted = 1 mm. (B) RT-PCR for *Fah* mRNA. Wild-type mRNA produces a 433-base pair fragment, whereas the exon-8-deleted mutant mRNA produces a shorter product. The bottom panel shows analysis of nine experimental samples at the left and controls at the right. A “ $\pm$ ” indicates whether reverse transcriptase was used. Samples 1-3 are from AAV-treated neonatal mice, samples 4 and 5 are from AAV-treated adults, and samples 6-9 are from serial transplant recipients.

different gene repair dynamics *in vivo*, d3  $Fah^{5981SB}$  neonates were treated with  $2 \times 10^{11}$  vg of AAV8-*Fah* or  $1 \times 10^{11}$  vg of AAV2-*Fah* and analyzed after 1, 2, or 4 weeks post-treatment for the presence of FAH<sup>+</sup> hepatocytes (Fig. 3). In AAV8-*Fah* treated mice, the highest number of FAH<sup>+</sup> hepatocytes seen (up to 1/180 hepatocytes) were detected within the first week post-treatment. Correction frequencies declined with time and stabilized after 4 weeks. In contrast, AAV2-treated mice had little detectable *Fah* expression within the first seven days, supporting the fact that AAV2 uncoats more slowly than AAV8. Week two showed an increase in *Fah* expression that remained stable until week four. No FAH<sup>+</sup> hepatocytes were detected at any time point in control mice injected with serotype-matched irrelevant control vectors AAV8-*GFP* or AAV2-*hAAT* at equivalent doses. These results conclusively demonstrate that emergence of FAH<sup>+</sup> hepatocytes were neither due to spontaneous reversion, nor gene repair stimulated non-specifically by mere AAV transduction.

**Gene Repair in Response to Different Vector Doses.** To examine dose responses, d3  $Fah^{5981SB}$  neonates were

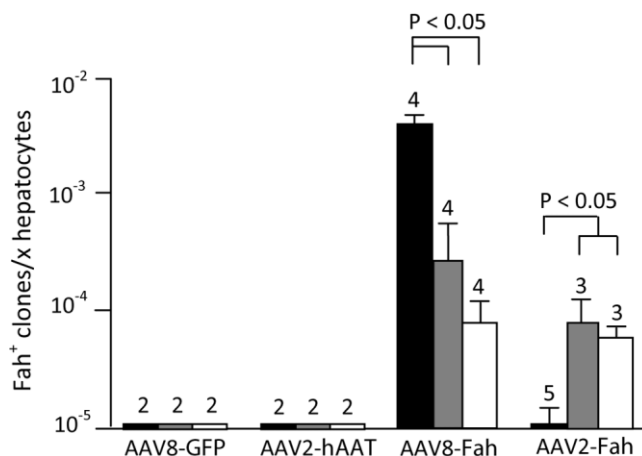


Fig. 3. Time-course study of AAV-mediated gene repair frequencies in neonates. Vectors are noted below each set and were administered at  $1 \times 10^{11}$  to  $2 \times 10^{11}$  vg. Frequencies were quantified by counting single FAH<sup>+</sup> clones per x hepatocytes (1/x) from neonates harvested 1, 2, or 4 weeks after treatment. Means  $\pm$  standard deviation are shown, with the number of animals analyzed indicated above each bar. Black bar = 1 week after treatment; gray bar = 2 weeks after treatment; white bar = 4 weeks after treatment.

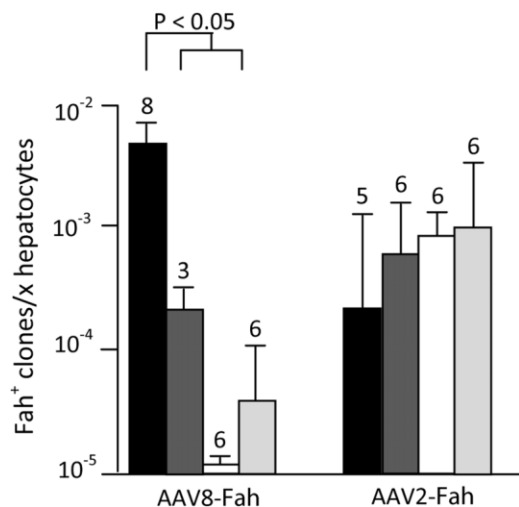


Fig. 4. Dose response study of AAV-mediated gene repair frequencies in neonates. Vectors administered are noted below each data set and were administered at  $3 \times 10^{11}$  to  $3 \times 10^8$  vg. Frequencies were quantified by counting single FAH<sup>+</sup> clones per x hepatocytes (1/x) from neonates harvested 3 weeks after treatment. Means  $\pm$  standard deviation are shown, with the number of animals analyzed indicated above each bar. Black bar =  $3 \times 10^{11}$  vg; dark gray bar =  $3 \times 10^{10}$  vg; white bar =  $3 \times 10^9$  vg; light gray bar =  $3 \times 10^8$  vg.

injected with four AAV-*Fah* concentrations ranging from  $3 \times 10^8$  to  $3 \times 10^{11}$  vg for each serotype and kept on NTBC until harvest at weaning to prevent metabolic selection of FAH<sup>+</sup> cells. In general, AAV8-*Fah* displayed a linear dose response over the range of doses administered (Fig. 4) where the highest doses administered produced the greatest gene repair. The difference in repair frequencies between the highest dose and all other doses admin-

istered was significant. In contrast, AAV2-*Fah* had no significant change in repair frequency over the entire range of doses administered. Overall, results indicate that AAV8-mediated gene repair is superior to that with AAV2.

**AAV-Mediated Gene Repair Is Feasible in Quiescent Liver.** The adult liver has considerably less cellular turnover than neonatal liver undergoing rapid growth and proliferation. Thus, gene repair frequencies are predicted to be lower in adults as homologous recombination is most prevalent during mitotic S-phase.<sup>37</sup> AAV8 was chosen to test the feasibility of gene repair in the nearly quiescent adult liver as it had now been demonstrated to be both faster and more efficient at gene repair than AAV2. Adult *Fah*<sup>5981SB</sup> mice (8-12 weeks old) were injected with  $1 \times 10^{11}$  vg of AAV8-*Fah* (n = 6), whereas age-matched littermate controls were injected with isotonic NaCl (n = 8). Mice were withdrawn from NTBC to allow selection of corrected hepatocytes. Serum for liver function tests and liver tissue were harvested >12 weeks after treatment. Mice treated with AAV8-*Fah* showed clinical improvement and repopulation with FAH<sup>+</sup> hepatocytes (Fig. 5A), whereas all mice in the control group had to be euthanized and showed no hepatic repopulation. Surprisingly, the initial correction frequency of FAH<sup>+</sup> nodules was comparable to that seen with neonatal administration. The clonal expansion of corrected hepatocytes was able to reverse the tyrosinemic phenotype and was highly reproducible. Liver function tests for AST and bilirubin demonstrated near complete correction when compared to controls (Fig. 5B).

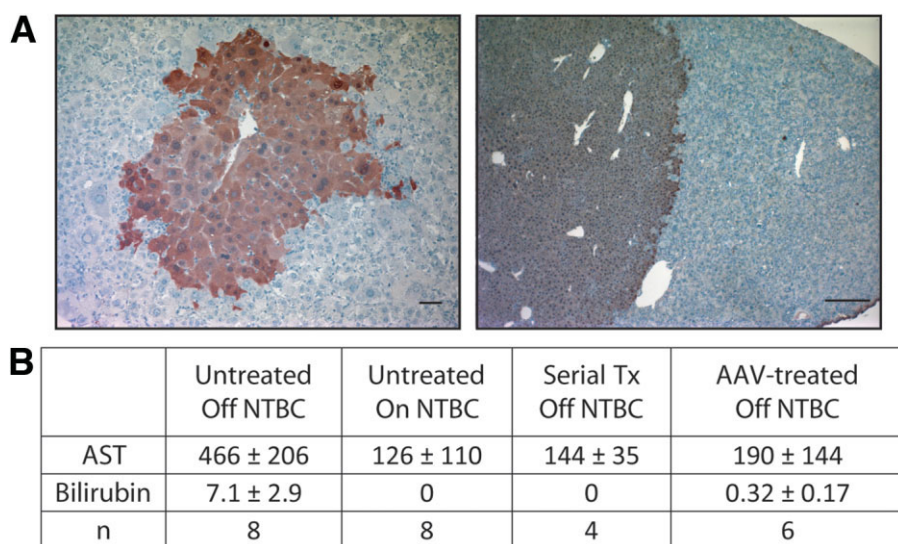


Fig. 5. AAV-mediated gene repair is feasible in adult liver. (A) Liver sections stained for FAH from adult *Fah*<sup>5981SB</sup> mice more than 12 weeks after treatment with AAV8-*Fah*. Scale bars = 100  $\mu$ m. (B) Liver function test results. Aspartate aminotransferase (AST [U/l]); bilirubin (mg/dL). Values ( $\pm$  standard deviation) represent adult untreated *Fah*<sup>5981SB</sup> mice off or on NTBC, serially transplanted (Tx) *Fah*<sup>5981SB</sup> mice off NTBC, and adult AAV-treated *Fah*<sup>5981SB</sup> mice off NTBC.

**Table 1. Frequency of Random Integration**

hAAT Copy Number in Recipient Mice			
Donor	sTx Recipient	Number of Copies/dGE	Average
1	1a	0.009	0.028 ± 0.023
	1b	0.026	
	1c	0.002	
	1d	0.042	
	1e	0.058	
2	2a	0.002	0
	2b	0.001	
	2c	0	
	2d	0	
	2e	0	
Total			0.005
Correction factor			2
Random integration			0.01 = 1%

After neonatal coinjection of  $4 \times 10^{10}$  vg of both AAV8-*Fah* and AAV8-*hAAT*, *FAH*<sup>+</sup> hepatocytes were selected for and then serially transplanted to remove any episomes. Data represent the number of copies of *hAAT* per diploid genome equivalent (dGE) in serial transplant (sTx) recipients. Because only 50% of the hepatocytes in these repopulated livers were derived from the original AAV-*Fah* treated donor liver, the frequency was corrected by a factor of 2 to give an estimated random integration frequency of 1%.

**Frequency of Random Integration.** Although phenotypic reversion of *Fah*<sup>5981SB</sup> mice indicates successful site-specific gene repair, random integration could also occur.<sup>38</sup> To assess random integration frequencies, d3 *Fah*<sup>5981SB</sup> neonates were coinjected with  $4 \times 10^{10}$  vg of AAV8-*Fah* and an irrelevant serotype-matched control vector AAV8-*hAAT*. Post-weaning, mice were subjected to NTBC withdrawal to select for corrected hepatocytes. To ensure no episomes remained,  $5 \times 10^5$  random hepatocytes were then serially transplanted into eight secondary *Fah*<sup>5981SB</sup> recipients. After >12 weeks off NTBC, serum and liver tissue were collected at harvest. qPCR was used to determine *Fah* and *hAAT* copy numbers in each mouse (Table 1). The frequency of randomly integrated *hAAT* ranged from 0 (undetectable) to 0.06/dGE and averaged 0.005/dGE. Only half the hepatocytes in repopulated livers were donor-derived, thus frequencies were corrected by a factor of two, resulting in an average random integration frequency of 0.01/dGE (1%) in corrected hepatocytes. This number is similar to multiple estimates of random integration of AAV8 from the literature.<sup>35</sup> Liver function tests in serially transplanted mice demonstrated near complete reconstitution by normalization of AST and bilirubin levels (Fig. 5B). Differences in serum AST and bilirubin levels were significant ( $P < 0.05$ ). In addition, in neonatal follow-ups 16 weeks post-treatment, no tumors were observed ( $n = 15$ , data not shown).

## Discussion

AAV has emerged as the vector of choice for gene repair as its single-stranded nature facilitates correction by homologous recombination. Numerous studies have demonstrated successful AAV-mediated gene repair to correct different mutation types *in vitro*.<sup>16,17</sup> In doing so, these studies provided the essential validation and framework for all AAV-mediated gene repair studies *in vivo*. Few publications exist demonstrating repair *in vivo*,<sup>39,40</sup> and they are hindered by the fact that they target clinically irrelevant marker mutations in exogenously provided transgenes like green fluorescent protein (GFP) or LacZ. One report has shown limited efficacy *in vivo* using a neonatal mouse model of the disease mucopolysaccharidosis type VII.<sup>15</sup> In that study, a single point mutation in the  $\beta$ -glucuronidase gene was corrected at frequencies of  $10^{-4}$  to  $10^{-5}$  using AAV2 and AAV6 at  $2 \times 10^{11}$  to  $6 \times 10^{11}$  vg doses. Nonetheless, the low correction frequencies were not therapeutic in treated mice, because no selective advantage exists for corrected hepatocytes in that model. This study differs from our own in several ways. Our study is the first to demonstrate the stability of gene correction in both adult and neonatal mice. In addition to AAV2, our study demonstrated greater correction using AAV8, the most hepatotropic of all the naturally occurring AAV serotypes. Furthermore, correction frequencies of up to  $10^{-3}$  as early as 3 weeks after treatment in adult mice were shown; rather than  $10^{-4}$  in 12–24 weeks after treatment in the previous study. Finally, our work tested a range of AAV doses from  $10^{11}$  to  $10^8$  vg and was able to demonstrate correction at all doses administered.

Numerous handicaps to AAV-mediated gene repair remain. Most notable is the low frequency of correction *in vivo*. To date, this frequency is too low to be of therapeutic value for many diseases. However, our work demonstrates that AAV-mediated gene repair has the capacity to be a real therapeutic alternative in a suitable selection-based disease. In hereditary tyrosinemia type I, corrected hepatocytes have a selective growth advantage and can clonally expand to restore liver function, even if the initial gene repair efficiency is low. While this situation is an exception, there are several disorders in which selection has been shown, including Fanconi's anemia,<sup>41</sup> the copper storage disorder Wilson's disease,<sup>42</sup> many bile-acid transporter defects,<sup>43</sup> and junctional epidermolysis bullosa<sup>44</sup> to name a few. If correction frequencies were increased even 10-fold, they would become clinically relevant for an even broader range of diseases. For example, it has been predicted that gene repair frequencies of  $10^{-2}$  would have therapeutic benefit in patients with hemophilia A.<sup>45</sup>



Our study establishes the utility of two different AAV serotypes (AAV8 and AAV2) for hepatic gene targeting of both adult and neonatal mice *in vivo*. Interestingly, the biology of these two serotypes differed considerably in terms of gene targeting. Different kinetics for the two serotypes have been described previously with gene addition approaches wherein higher doses of AAV correlated with higher levels of gene expression.<sup>36</sup> Here, we observed a similar phenomenon where the highest doses administered produced the greatest gene repair frequencies *in vivo*. Targeting was confirmed by immunohistochemistry, RT-PCR, and functional measures of liver correction using serum liver function tests.

We also evaluated the frequency of random integration in cells with proper gene repair using coinjection with a second, nonselectable AAV vector. The average copy number of the irrelevant vector corrected for repopulation efficiency indicated that 0.5%-1% of targeted cells also had a random integration. This number is similar to multiple estimates of random integration of AAV8 from the literature.<sup>35</sup> Therefore, it can be concluded that gene repair does not result in a higher random integration frequency.

In summary, our experiments demonstrated stable hepatic gene repair in both adult and neonatal mice with AAV-*Fah* serotypes 2 and 8. Serial transplantation was possible without difficulty and serially reconstituted animals had normal hepatic function. Most importantly, this work was the first to show functional metabolic correction of a disease model using AAV-mediated gene repair and can be envisioned as a therapeutic strategy for disorders with a selective advantage in corrected cells. Although these experiments focused on correcting the metabolic disease HTI, the novel approach described herein can serve as a model for gene repair in any monogenic disease caused by point mutations.

**Acknowledgment:** We thank Angela Major for histology support and Terry Storm for AAV preparations.

## References

- Mueller C, Flotte TR. Clinical gene therapy using recombinant adeno-associated virus vectors. *Gene Ther* 2008;15:858-863.
- Russell DW, Kay MA. Adeno-associated virus vectors and hematology. *Blood* 1999;94:864-874.
- Hendrie PC, Hirata RK, Russell DW. Chromosomal integration and homologous gene targeting by replication-incompetent vectors based on the autonomous parvovirus minute virus of mice. *J Virol* 2003;77:13136-13145.
- Garrick D, Fiering S, Martin DI, Whitelaw E. Repeat-induced gene silencing in mammals. *Nat Genet* 1998;18:56-59.
- Donsante A, Miller DG, Li Y, Vogler C, Brunt EM, Russell DW, et al. AAV vector integration sites in mouse hepatocellular carcinoma. *Science* 2007;317:477.
- Verma IM, Somia N. Gene therapy—promises, problems and prospects. *Nature* 1997;389:239-242.
- Andrieu-Soler C, Halhal M, Boatright JH, Padove SA, Nickerson JM, Stodulkova E, et al. Single-stranded oligonucleotide-mediated *in vivo* gene repair in the rd1 retina. *Mol Vis* 2007;13:692-706.
- Huen MS, Lu LY, Liu DP, Huang JD. Active transcription promotes single-stranded oligonucleotide mediated gene repair. *Biochem Biophys Res Commun* 2007;353:33-39.
- Wu XS, Xin L, Yin WX, Shang XY, Lu L, Watt RM, et al. Increased efficiency of oligonucleotide-mediated gene repair through slowing replication fork progression. *Proc Natl Acad Sci U S A* 2005;102:2508-2513.
- Vasquez KM, Narayanan L, Glazer PM. Specific mutations induced by triplex-forming oligonucleotides in mice. *Science* 2000;290:530-533.
- Kren BT, Parashar B, Bandyopadhyay P, Chowdhury NR, Chowdhury JR, Steer CJ. Correction of the UDP-glucuronosyltransferase gene defect in the Gunn rat model of Crigler-Najjar syndrome type I with a chimeric oligonucleotide. *Proc Natl Acad Sci U S A* 1999;96:10349-10354.
- Kren BT, Bandyopadhyay P, Steer CJ. *In vivo* site-directed mutagenesis of the factor IX gene by chimeric RNA/DNA oligonucleotides. *Nat Med* 1998;4:285-290.
- Vasileva A, Jessberger R. Precise hit: adeno-associated virus in gene targeting. *Nat Rev Microbiol* 2005;3:837-847.
- Russell DW, Hirata RK. Human gene targeting by viral vectors. *Nat Genet* 1998;18:325-330.
- Miller DG, Wang PR, Petek LM, Hirata RK, Sands MS, Russell DW. Gene targeting *in vivo* by adeno-associated virus vectors. *Nat Biotechnol* 2006;24:1022-1026.
- Inoue N, Dong R, Hirata RK, Russell DW. Introduction of single base substitutions at homologous chromosomal sequences by adeno-associated virus vectors. *Mol Ther* 2001;3:526-530.
- Inoue N, Hirata RK, Russell DW. High-fidelity correction of mutations at multiple chromosomal positions by adeno-associated virus vectors. *J Virol* 1999;73:7376-7380.
- Hendrie PC, Russell DW. Gene targeting with viral vectors. *Mol Ther* 2005;12:9-17.
- Parekh-Olmedo H, Ferrara L, Brachman E, Kmiec EB. Gene therapy progress and prospects: targeted gene repair. *Gene Ther* 2005;12:639-646.
- Bergeron B. *Case Studies in Genes and Disease*. 1st ed. Philadelphia: American College of Physicians Press; 2004.
- Mitchell GA, Grompe M, Lambert M, Tanguay R. Hypertyrosinemia. In: *The Metabolic and Molecular Basis of Inherited Disease*. 8th ed. New York: McGraw-Hill; 2001:1777-1805.
- Grompe M. The pathophysiology and treatment of hereditary tyrosinemia type 1. *Semin Liver Dis* 2001;21:563-571.
- Al-Dhalimy M, Overturf K, Finegold M, Grompe M. Long-term therapy with NTBC and tyrosine-restricted diet in a murine model of hereditary tyrosinemia type I. *Mol Genet Metab* 2002;75:38-45.
- Overturf K, Al-Dhalimy M, Tanguay R, Brantly M, Ou CN, Finegold M, et al. Hepatocytes corrected by gene therapy are selected *in vivo* in a murine model of hereditary tyrosinaemia type I. *Nat Genet* 1996;12:266-273.
- Aponte JL, Sega GA, Hauser LJ, Dhar MS, Withrow CM, Carpenter DA, et al. Point mutations in the murine fumarylacetoacetate hydrolase gene: Animal models for the human genetic disorder hereditary tyrosinemia type 1. *Proc Natl Acad Sci U S A* 2001;98:641-645.
- Culiat CT, Klebig ML, Liu Z, Monroe H, Stanford B, Desai J, et al. Identification of mutations from phenotype-driven ENU mutagenesis in mouse chromosome 7. *Mamm Genome* 2005;16:555-566.
- Grompe M, Lindstedt S, al-Dhalimy M, Kennaway NG, Papaconstantinou J, Torres-Ramos CA, et al. Pharmacological correction of neonatal lethal hepatic dysfunction in a murine model of hereditary tyrosinaemia type I. *Nat Genet* 1995;10:453-460.
- Nakai H, Montini E, Fuess S, Storm TA, Meuse L, Finegold M, et al. Helper-independent and AAV-ITR-independent chromosomal integration of double-stranded linear DNA vectors in mice. *Mol Ther* 2003;7:101-111.



29. Sands MS, Barker JE. Percutaneous intravenous injection in neonatal mice. *Comp Med* 2000;50:107.
30. Chen ZY, Yant SR, He CY, Meuse L, Shen S, Kay MA. Linear DNAs concatemerize in vivo and result in sustained transgene expression in mouse liver. *Mol Ther* 2001;3:403-410.
31. Grimm D, Pandey K, Nakai H, Storm TA, Kay MA. Liver transduction with recombinant adeno-associated virus is primarily restricted by capsid serotype not vector genotype. *J Virol* 2006;80:426-439.
32. Mitchell C, Willenbring H. A reproducible and well-tolerated method for 2/3 partial hepatectomy in mice. *Nat Protoc* 2008;3:1167-1170.
33. Wang X, Montini E, Al-Dhalimy M, Lagasse E, Finegold M, Grompe M. Kinetics of liver repopulation after bone marrow transplantation. *Am J Pathol* 2002;161:565-574.
34. Grimm D, Kay MA, Kleinschmidt JA. Helper virus-free, optically controllable, and two-plasmid-based production of adeno-associated virus vectors of serotypes 1 to 6. *Mol Ther* 2003;7:839-850.
35. Nakai H, Montini E, Fuess S, Storm TA, Grompe M, Kay MA. AAV serotype 2 vectors preferentially integrate into active genes in mice. *Nat Genet* 2003;34:297-302.
36. Thomas CE, Storm TA, Huang Z, Kay MA. Rapid uncoating of vector genomes is the key to efficient liver transduction with pseudotyped adeno-associated virus vectors. *J Virol* 2004;78:3110-3122.
37. Cahill D, Connor B, Carney JP. Mechanisms of eukaryotic DNA double strand break repair. *Front Biosci* 2006;11:1958-1976.
38. Nakai H, Wu X, Fuess S, Storm TA, Munroe D, Montini E, et al. Large-scale molecular characterization of adeno-associated virus vector integration in mouse liver. *J Virol* 2005;79:3606-3614.
39. Vijg J, Dolle ME, Martus HJ, Boerigter ME. Transgenic mouse models for studying mutations in vivo: applications in aging research. *Mech Ageing Dev* 1997;98:189-202.
40. Nickerson HD, Colledge WH. A LacZ-based transgenic mouse for detection of somatic gene repair events in vivo. *Gene Ther* 2004;11:1351-1357.
41. Battaile KP, Bateman RL, Mortimer D, Mulcahy J, Rathbun RK, Bagby G, et al. In vivo selection of wild-type hematopoietic stem cells in a murine model of Fanconi anemia. *Blood* 1999;94:2151-2158.
42. Allen KJ, Cheah DM, Wright PF, Gazeas S, Pettigrew-Buck NE, Deal YH, et al. Liver cell transplantation leads to repopulation and functional correction in a mouse model of Wilson's disease. *J Gastroenterol Hepatol* 2004;19:1283-1290.
43. De Vree JM, Ottenhoff R, Bosma PJ, Smith AJ, Aten J, Oude Elferink RP. Correction of liver disease by hepatocyte transplantation in a mouse model of progressive familial intrahepatic cholestasis. *Gastroenterology* 2000;119:1720-1730.
44. Ortiz-Urda S, Lin Q, Yant SR, Keene D, Kay MA, Khavari PA. Sustainable correction of junctional epidermolysis bullosa via transposon-mediated nonviral gene transfer. *Gene Ther* 2003;10:1099-1104.
45. Kay MA, High K. Gene therapy for the hemophilias. *Proc Natl Acad Sci U S A* 1999;96:9973-9975.